EPJ Web of Conferences **80**, 00004 (2014)
DOI: 10.1051/epjconf/20148000004
© Owned by the authors, published by EDP Sciences, 2014

Latest LHCb results

Maurizio Martinelli[1,a] on behalf the LHCb collaboration

[1] *École polytechnique fédéral de Lausanne*

Abstract. The LHCb experiment is one of the major research projects at the Large Hadron Collider. Its acceptance and instrumentation is optimised to perform high-precision studies of flavour physics and particle production in a unique kinematic range at unprecedented collision energies. Using large data samples accumulated in the years 2010-2012, the LHCb collaboration has conducted a series of measurements providing a sensitive test of the Standard Model and strengthening our knowledge of flavour physics, QCD and electroweak processes. The status of the experiment and some of its recent results are presented here.

1 The LHCb experiment

The LHCb experiment is one of the major research projects at the Large Hadron Collider (LHC). It is designed for detecting particles containing b and c quarks and search for phenomena beyond the Standard Model (SM) in the heavy flavour sector. Since b and c quarks are produced mostly in the forward or backward regions at the LHC, LHCb is a forward detector covering about 4% of the total solid angle ($2 < \eta < 5$), which corresponds to 40% of the total $b\bar{b}$ and $c\bar{c}$ cross-section. The detector recorded about $3\,\text{fb}^{-1}$ of pp collisions in the three years of data collection, between 2010 and 2012, at center-of-mass energies of 7 TeV and 8 TeV.

The layout of the LHCb detector is shown in Fig. 1. It includes a high-precision tracking system consisting of a silicon-strip vertex detector surrounding the pp interaction region [1], a large-area silicon-strip detector located upstream of a dipole magnet with a bending power of about 4 Tm, and three stations of silicon-strip detectors and straw drift tubes [2] placed downstream of the magnet. The tracking system provides a measurement of momentum, p, with a relative uncertainty that varies from 0.4% at low momentum to 0.6% at 100 GeV/c. The minimum distance of a track to a primary vertex, the impact parameter, is measured with a resolution of $(15 + 29/p_{\text{T}})\,\mu\text{m}$, where p_{T} is the component of p transverse to the beam, in GeV/c. Different types of charged hadrons are distinguished using information from two ring-imaging Cherenkov detectors [3]. Photon, electron and hadron candidates are identified by a calorimeter system consisting of scintillating-pad and preshower detectors, an electromagnetic calorimeter and a hadronic calorimeter. Muons are identified by a system composed of alternating layers of iron and multiwire proportional chambers [4]. The trigger [5] consists of a hardware stage, based on information from the calorimeter and muon systems, followed by a software stage, which applies a full event reconstruction.

[a] e-mail: maurizio.martinelli@epfl.ch

This is an Open Access article distributed under the terms of the Creative Commons Attribution License 4.0, which permits unrestricted use, distribution, and reproduction in any medium, provided the original work is properly cited.

Article available at http://www.epj-conferences.org or http://dx.doi.org/10.1051/epjconf/20148000004

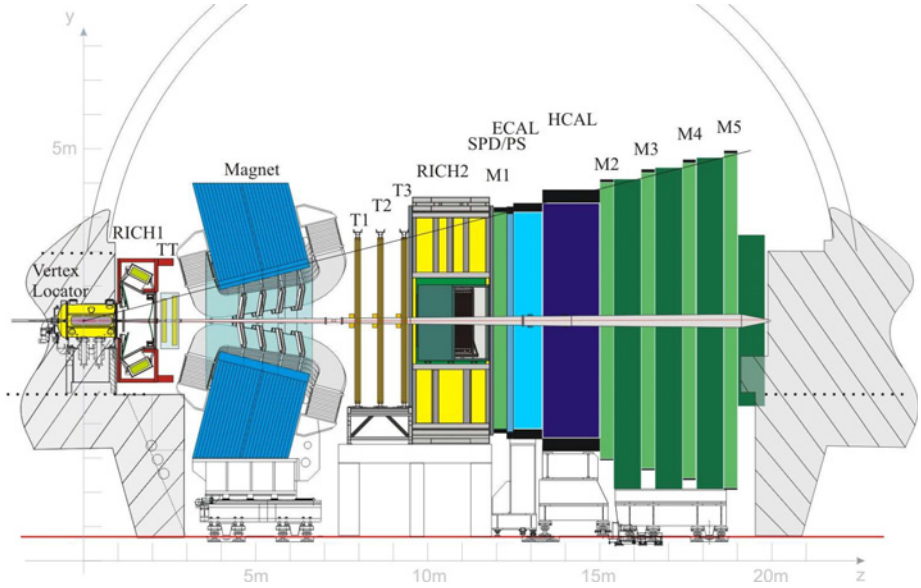

Figure 1. Overview of the LHCb detector

2 Selected physics results

The LHCb physics case spans a wide range of topics, from high-precision *CP* violation measurements, to the search for new exotic particles, to cross-section measurements. In the following a few selected results are shown.

2.1 Exotic particles

One of the major results published recently is the confirmation of the $Z^+(4430)$ resonance in $B^0 \to J/\psi K^+\pi^-$ decays [6]. Its minimal quark content of $c\bar{c}d\bar{u}$ makes it a clear exotic state, for which tetraquark and molecular hypotheses have been made. The existence of this state has been debated since its first evidence by the Belle collaboration [7] and the non-conclusive BaBar results [8].

The LHCb analysis uses model-independent and model-dependent techniques to exploit the full potential of the data. The results of the two approaches are shown in Fig. 2. Both approaches do not allow the data to be described adequately without including the $Z^+(4430)$ resonance. The four-dimensional model-dependent fit allows to measure the mass $m = 4475 \pm 7^{+15}_{-25}\,\mathrm{MeV}/c^2$ and the width $\Gamma = 172 \pm 13^{+37}_{-34}\,\mathrm{MeV}/c^2$ of the resonance, and to exclude the $J^P = 0^-$ spin hypothesis in favour of the 1^+ with exceedingly large significance. An Argand diagram of the observed peak confirms its resonant structure. Indications for the presence of another resonant structure at a mass of about $4.1\,\mathrm{GeV}/c^2$ have been considered, but the Argand plot is not conclusive in this case. Further analysis will be pursued once larger data samples will be available.

Another decay mode that recently provided insights on exotic particles is $B^0 \to J/\psi\pi^+\pi^-$ [9]. From this decay mode, exact information about the substructure of light mesons decaying to $\pi^+\pi^-$ can be extracted. Considerations on the tetraquark nature of the $f_0(500)$ and $f_0(980)$ are made by studying the relative branching ratios of $B^0 \to J/\psi\, f_0(980)$ and $B^0 \to J/\psi\, f_0(500)$. Stone et al. [10] have argued that if these two states are tetraquarks, this ratio should be exactly 0.5.

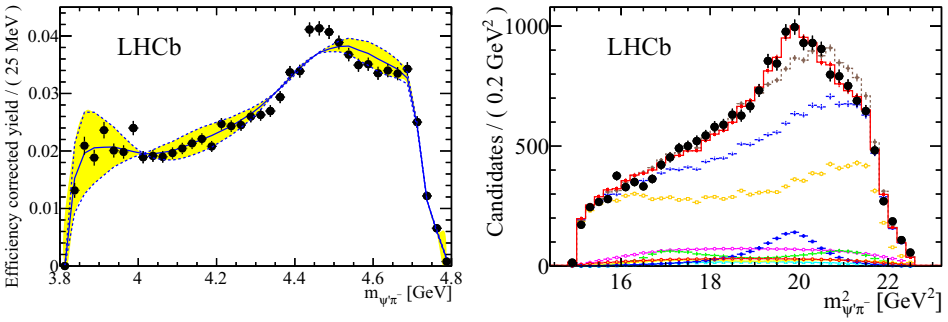

Figure 2. The projection on the $\psi\pi^-$ invariant mass of the results of a model-independent analysis of the $B^0 \to J/\psi\, K^+\pi^-$ decays are shown on the left. Similarly, the results of a model-dependent fit to the data are shown on the right including the $Z^+(4430)$ resonance (red) and excluding it (brown). Reflections from other resonant contributions decaying to $K^+\pi^-$ are shown with different colours.

An angular analysis is needed for extracting this information, therefore the distribution of the events is studied in the four-dimensional space defined by the $\pi^+\pi^-$ invariant mass, the cosine of the muon (pion) helicity angle in the J/ψ ($\pi^+\pi^-$) rest-frame $\cos\theta_{J/\psi}$ ($\cos\theta_{\pi^+\pi^-}$), and the angle χ between the decaying planes of the two pions and the two muons. About 18,000 events have been selected in 3 fb^{-1} data. The fit used to extract the B^0 signal contribution is shown in Fig. 3 alongside the projections of the fit results on the $\pi^+\pi^-$ invariant mass spectrum. The fit required six interfering states

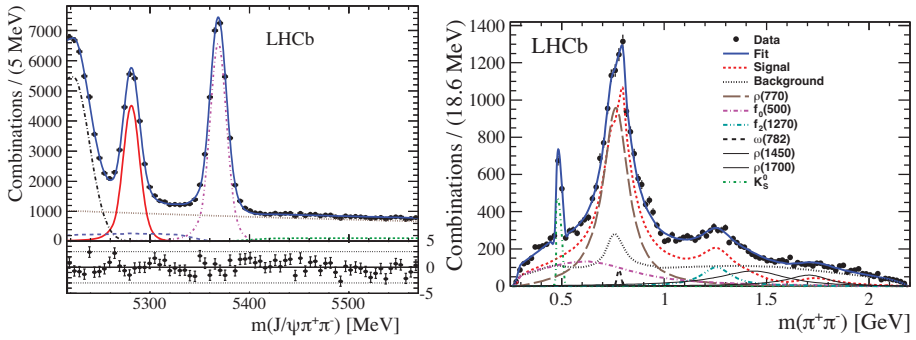

Figure 3. Signal events distribution (red line) is extracted from a fit to the $J/\psi\,\pi^+\pi^-$ invariant mass distribution (left). The projection of the fit results on the $\pi^+\pi^-$ invariant mass are shown on the right.

to converge, among which the $f_0(980)$ was not found. A limit is set on the mixing angle between the $f_0(500)$ and $f_0(980)$, $\phi_m < 17^\circ$ at 90% confidence level.

2.2 Rare decays

The LHCb experiment has a wide program for measuring properties or rare decays of B mesons. In particular, many decays regulated by flavour changing neutral currents are studied. These decays are rare in the SM because they are mediated by penguin or loop diagrams. This characteristic makes

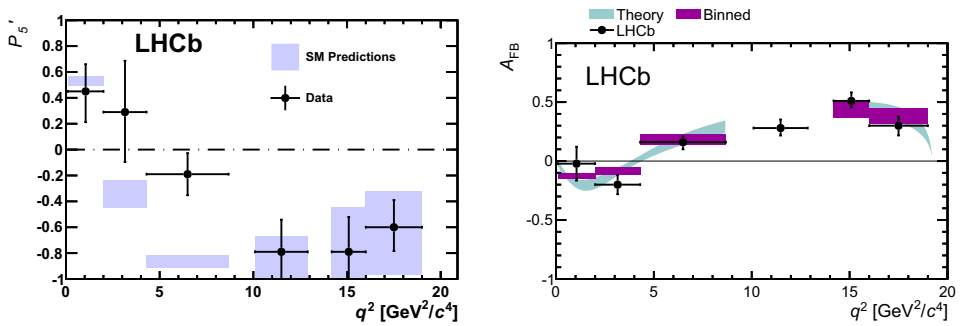

Figure 4. The measured values of P_5' are compared with the SM predictions on the left. The forward-backward asymmetry is shown on the right with the LHCb measurement overlaid to the SM predictions.

them particularly sensitive to beyond-the-SM (BSM) processes that could affect their decay rates, angular observables, and *CP* asymmetries.

The most famous of these decay modes is probably the $B_s^0 \to \mu^+\mu^-$ decay. Its branching ratio is precisely predicted in the SM to be $\mathcal{B}(B_s^0 \to \mu^+\mu^-) = (3.65 \pm 0.23) \times 10^{-9}$ [11]. Such a small branching ratio is due to GIM and helicity suppressions in the SM. Processes beyond the SM could contribute by enhancing this branching ratio, for example through the mediation of new particles from an extended Higgs sector. The LHCb [12] and CMS [13] experiments, studying the whole data sample collected in 2011 and 2012, found evidence of this B_s^0 decay with a rate consistent with the SM, placing strong constraints to BSM effects.

Further searches for effects of BSM physics are made through the $B^0 \to K^{*0}\mu^+\mu^-$ decay mode. A large set of observables is studied for comparing the results with the SM predictions. In Fig. 4, the results of the LHCb analysis on the data collected in 2011 are shown [14, 15]. A large local discrepancy in the form-factor-independent angular observable P_5' is observed, while the forward-backward asymmetry $A_{\rm FB}$ is found to be consistent with the SM predictions. This analysis requires more data to establish the discrepancy and will be soon updated with the addition of the 2012 data sample. Nevertheless, it stimulated a wide theoretical interest, since such discrepancy is difficult to explain within SUSY scenarios [16], and is consistent to a Z' boson with 7 TeV mass [17]. Other authors suggest that this is due to the underestimation of theoretical uncertainties [18, 19].

Another $b \to s$ loop transition that has been recently investigated by the LHCb involves photons. The photon produced after the $b \to s\gamma$ loop diagram is predominantly left-handed, since the recoiling s quark that couples to the W boson is left-handed. Within the SM, maximal parity violation holds up to within a few percent. Processes beyond the SM, could let the photon acquire an appreciable right-handed component due to the chirality flip along a heavy fermion line in the electroweak loop process. For example, due to left-right W boson or s quark mixing.

The photon polarisation in $b \to s\gamma$ transitions has been studied in LHCb through the $B^+ \to K^+\pi^+\pi^-\gamma$ decay mode [20]. The measurement is conceptually similar to the Wu measurement of parity violation [21], but in this case the polarisation angle of the photon is measured with respect to the normal to the plane of the K^* daughters. Unpolarised photons would show no asymmetry. Using data collected in 2011 and 2012, about 14,000 B^+ decays have been identified. The $K^+\pi^+\pi^-$ invariant mass spectrum is then studied and found rich of resonant states. Contributions from $K_1(1270)^+$, $K_1(1400)^+$, $K_2^*(1430)^+$, and $K^*(1410)^+$ are clearly present as shown in Fig. 5. The $K^+\pi^+\pi^-$ invariant mass spectrum is divided into four regions associated to various resonance contributions, and the

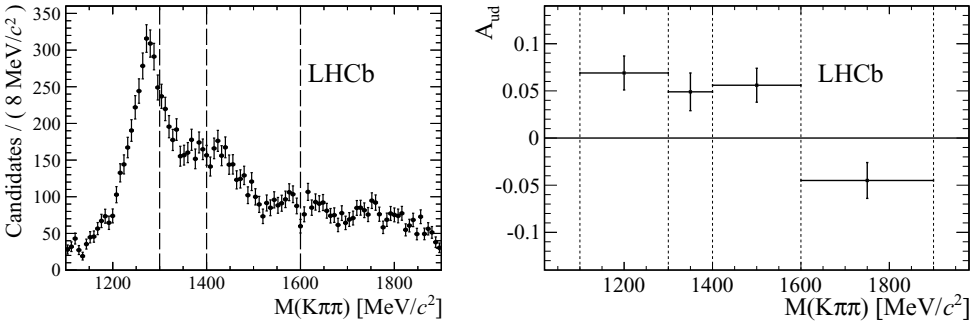

Figure 5. The $K^+\pi^+\pi^-$ invariant mass spectrum for $B^+ \to K^+\pi^+\pi^-\gamma$ decays is shown on the left. The four different regions in which up-down asymmetry is measured are separated by dashed lines. The up-down asymmetry for each of these four regions is shown on the right.

photon polarisation asymmetry is measured in each of them. The photon polarisation is described by means of the distribution of the polarisation angle $\hat{\theta}$, that is the angle described by photon direction with respect to the $K^+\pi^+\pi^-$ decay plane. The distribution of events in $\cos\hat{\theta}$ is parametrised by using a linear expansion of Legendre polynomials up to the 4^{th} power. By considering the asymmetry measured in the four regions, this analysis provides the first observation of photon polarisation with a significance of 5.2 standard deviations.

2.3 Charm physics

A large sample of charmed hadrons is produced within the LHCb acceptance as well. It was natural for the LHCb collaboration to develop a wide program for studying charm decays at the LHC. The search for *CP* violation in the charm sector is one of the most interesting topics in this field. *CP* violation is expected to be suppressed at $O(10^{-3})$ in the SM due to the small amplitude of the Cabibbo-Kobayashi-Maskawa matrix elements involved. One simple way to obtain *CP* violation in charm decays is through the interference of the tree and penguin diagrams in Cabibbo suppressed $c \to uq\bar{q}$ decays. Such processes are sensitive to effects of BSM particles, that could enhance *CP* violation up to the percent level. The experimental sensitivity at LHCb is at $O(10^{-3})$, which allows possible effects to be observed.

The most sensitive analysis for *CP* violation in Charm is the measurement of $\Delta A_{CP} = A_{CP}(D^0 \to K^+K^-) - A_{CP}(D^0 \to \pi^+\pi^-)$ [22]. In the limit of *U*-spin symmetry the *CP* violating asymmetry should be opposite in $D^0 \to K^+K^-$ and $D^0 \to \pi^+\pi^-$. Therefore, the observation of $\Delta A_{CP} \neq 0$ would be a signal of *CP* violation in at least one of the two decay modes considered. Using D^0 originating from semileptonic B decays, about 2,000,000 $D^0 \to K^+K^-$ and 700,000 $D^0 \to \pi^+\pi^-$ decays are reconstructed in 3 fb^{-1} of data (see Fig. 6), corresponding to a sensitivity on ΔA_{CP} of 0.16%.

Even if the muon detection and B production asymmetries cancel in the difference between $A_{CP}^{\text{meas}}(D^0 \to K^+K^-)$ and $A_{CP}^{\text{meas}}(D^0 \to \pi^+\pi^-)$, the *CP* violating asymmetry cannot be directly compared between the two due to acceptance effects. These effects are corrected by applying weights to one of the two samples such that the transverse momentum and pseudorapidity distributions of the D^0 match between the two. Once the corrections are applied, the value $\Delta A_{CP} = (+0.14 \pm 0.16\,(\text{stat}) \pm 0.08\,(\text{syst}))\%$ is obtained. This result shows no *CP* violation up to the level of 0.2% and is currently the best limit for *CP* violation in charm decays.

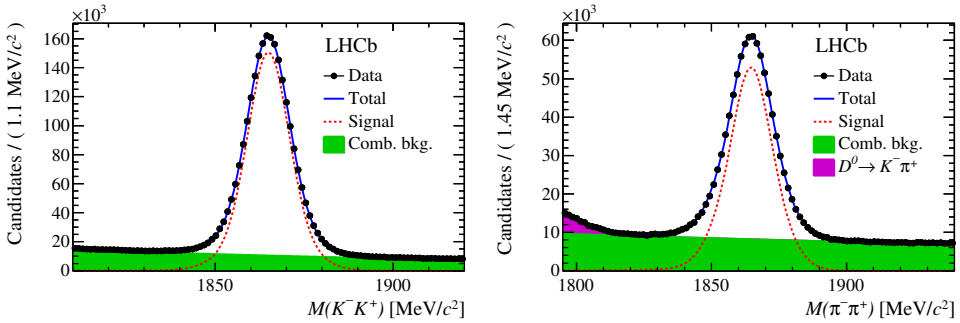

Figure 6. The invariant mass spectrum for $D^0 \to K^+K^-(\pi^+\pi^-)$ decays is shown on the left (right). The results of the fit are overlaid to the data point with a blue solid line. A red dashed line shows the projection of the signal distribution. A green-filled area represents the combinatorial background and the purple-filled one the background from Cabibbo-favoured $D^0 \to K^-\pi^+$ decays in which the kaon has been misreconstructed as a pion.

In the same analysis, $A_{CP}(D^0 \to K^+K^-)$ and $A_{CP}(D^0 \to \pi^+\pi^-)$ are also measured. The Cabibbo-favoured $D^0 \to K^-\pi^+$ decay from semileptonic B decays is used to correct for the muon detection and B production asymmetries. Since the detector introduces a spurious asymmetry on the reconstruction of $K^-\pi^+$ and $K^+\pi^-$ pairs, prompt $D^+ \to K^-\pi^+\pi^+$ decays are used to correct for it. This in turn introduces D^+ and π^+ detection asymmetries that are corrected by prompt $D^+ \to \overline{K}^0\pi^+$ decays. The remaining $\overline{K}^0$ detection asymmetry is corrected by using calculations of the expected asymmetry from K^0-$\overline{K}^0$ mixing and regeneration effects in the LHCb detector. The *CP* violating asymmetries are found to be $A_{CP}(D^0 \to K^+K^-) = (-0.06 \pm 0.15\,(\text{stat}) \pm 0.10\,(\text{syst}))\%$ and $A_{CP}(D^0 \to \pi^+\pi^-) = (-0.20 \pm 0.19\,(\text{stat}) \pm 0.10\,(\text{syst}))\%$, respectively, and show no sign of *CP* violation so far.

Another high-sensitivity measurement recently published by the LHCb collaboration uses $D^+_{(s)} \to K^0_S h^+$ decays, where $h = K, \pi$ [23]. In this case, the Cabibbo-suppressed decay modes are $D^+ \to K^0_S K^+$ and $D^+_s \to K^0_S\pi^+$, and the Cabibbo-favoured $D^+_s \to K^0_S K^+$ and $D^+ \to K^0_S\pi^+$ decays are used for $D^+_{(s)}$ production and π/K detection asymmetry corrections. The K^0-$\overline{K}^0$ regeneration and material interaction asymmetries are estimated analytically. The events reconstructed in 3 fb^{-1} of LHCb data are shown in Fig. 7. A similar procedure to that outlined above is used to correct for the $D^+_{(s)}$ production and π/K detection asymmetry. The results are $A_{CP}(D^+ \to K^0_S K^+) = (+0.03 \pm 0.17\,(\text{stat}) \pm 0.14\,(\text{syst}))\%$ and $A_{CP}(D^+_s \to K^0_S\pi^+) = (+0.38 \pm 0.46\,(\text{stat}) \pm 0.17\,(\text{syst}))\%$. No sign of *CP* violation is observed yet.

3 Future prospects

In 2015 the LHC will deliver pp collisions with an increased center-of-mass energy of 13 TeV. The LHCb experiment plans to record about 2 fb^{-1} of data per year in order to collect 10 fb^{-1} of data by the end of the second run of the LHC in 2018. Afterwards, a second long period of LHC shutdown is planned, during which the LHCb collaboration will install upgraded components [24, 25].

Major improvements will be delivered on both trigger and tracking sides. All detectors will feature a 40 MHz readout (thus matching the LHC bunch crossing rate), and the online computing farm will be significantly upgraded. These upgrades will allow a fully software-based trigger to be operated at much higher rates. The vertex locator and all tracking stations will be upgraded to detector technologies best suited for the large expected track multiplicity. Silicon pixel detectors will be used

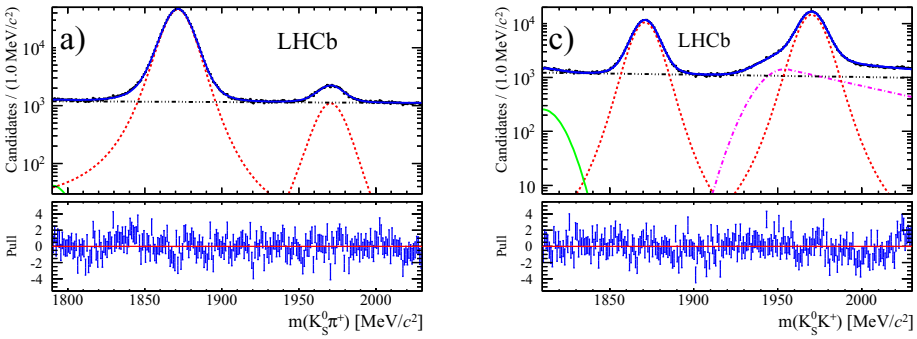

Figure 7. The invariant mass spectrum of $K^0_S\pi^+(K^0_SK^+)$ decays is shown on the left (right). The results of the fit are overlaid to the data point with a blue solid line. A red dashed line shows the projection of the D^+ and D^+_s signal distributions. The combinatorial background is shown by a dash-dotted blue line. A solid green line represents the background from $D^+ \to K^0_S\pi^+\pi^0$ in the left plot and $D^+_s \to K^+K^-\pi^+\pi^0$ in the right plot. The magenta dash-dotted line represents the background from Cabibbo-favoured $D^+_{(s)} \to K^0_S\pi^+(K^0_SK^+)$ decays in which the pion (kaon) has been misreconstructed as a kaon (pion).

for the vertex locator, the silicon strips tracking stations upstream the magnet will be redesigned to enlarge the acceptance of the sub-detector at high pseudorapidity, and the downstream tracking stations will use scintillating fibres to maintain the same excellent tracking performance of LHCb in the high-multiplicity environment.

The LHCb upgraded detector will record $10\,\text{fb}^{-1}$ of data per year, and the plan is to record at least $50\,\text{fb}^{-1}$ in total. These data will allow to perform measurements of several key observables with unprecedented sensitivity [26].

4 Conclusions

The LHCb detector performed very well during the 2011 and 2012 data-taking periods, allowing the collaboration to produce many interesting results with the best sensitivity to date.

The analysis of the events collected during the 2011 and 2012 runs of the LHC is not yet over, and there are new searches and updates foreseen in the next future. Most of the LHCb results have very small systematic uncertainties, therefore significant improvements are expected with the addition of more data.

The LHCb experiment has just started to probe the SM with unprecedented precision in many physics decay channels. The addition of data in the coming years and the LHCb Upgrade will improve the sensitivity of the experiment towards uncertainties comparable to those from the most precise theoretical calculations, providing the most powerful searches for BSM effects.

References

[1] R. Aaij *et al.*, arXiv:1405.7808 [physics.ins-det].
[2] R. Arink *et al.*, JINST **9**, 01002 (2014) [arXiv:1311.3893 [physics.ins-det]].
[3] M. Adinolfi *et al.*, Eur. Phys. J. C **73**, 2431 (2013) [arXiv:1211.6759 [physics.ins-det]].
[4] A. A. Alves, Jr. *et al.*, JINST **8**, P02022 (2013) [arXiv:1211.1346 [physics.ins-det]].

[5] R. Aaij *et al.*, JINST **8**, P04022 (2013) [arXiv:1211.3055 [hep-ex]].
[6] R. Aaij *et al.*, Phys. Rev. Lett. **112**, 222002 (2014) [arXiv:1404.1903 [hep-ex]].
[7] S. K. Choi *et al.*, Phys. Rev. Lett. **100**, 142001 (2008) [arXiv:0708.1790 [hep-ex]].
[8] B. Aubert *et al.*, Phys. Rev. D **79**, 112001 (2009) [arXiv:0811.0564 [hep-ex]].
[9] R. Aaij *et al.*, Phys. Rev. D **90**, 012003 (2014) [arXiv:1404.5673 [hep-ex]].
[10] S. Stone and L. Zhang, Phys. Rev. Lett. **111**, no. 6, 062001 (2013) [arXiv:1305.6554 [hep-ex]].
[11] C. Bobeth *et al.*, Phys. Rev. Lett. **112**, 101801 (2014) [arXiv:1311.0903 [hep-ph]].
[12] R. Aaij *et al.*, Phys. Rev. Lett. **111**, 101805 (2013) [arXiv:1307.5024 [hep-ex]].
[13] S. Chatrchyan *et al.*, Phys. Rev. Lett. **111**, 101804 (2013) [arXiv:1307.5025 [hep-ex]].
[14] R. Aaij *et al.* [LHCb Collaboration], JHEP **1308**, 131 (2013) [arXiv:1304.6325 [hep-ex]].
[15] R. Aaij *et al.*, Phys. Rev. Lett. **111**, 191801 (2013) [arXiv:1308.1707 [hep-ex]].
[16] W. Altmannshofer and D. M. Straub, Eur. Phys. J. C **73**, 2646 (2013) [arXiv:1308.1501 [hep-ph]].
[17] D. M. Straub, JHEP **1308**, 108 (2013) [arXiv:1302.4651 [hep-ph]].
[18] F. Beaujean *et al.*, Eur. Phys. J. C **74**, 2897 (2014) [arXiv:1310.2478 [hep-ph]].
[19] S. Jäger and J. Martin Camalich, JHEP **1305**, 043 (2013) [arXiv:1212.2263 [hep-ph]].
[20] R. Aaij *et al.*, Phys. Rev. Lett. **112**, 161801 (2014) [arXiv:1402.6852 [hep-ex]].
[21] C. S. Wu *et al.*, Phys. Rev. **105**, 1413 (1957).
[22] R. Aaij *et al.*, JHEP **1407**, 041 (2014) [arXiv:1405.2797 [hep-ex]].
[23] R. Aaij *et al.*, arXiv:1406.2624 [hep-ex].
[24] R. Aaij *et al.*, *Letter of Intent for the LHCb Upgrade*, CERN-LHCC-2011-001 (2011).
[25] R. Aaij *et al.*, *Framework TDR for the LHCb Upgrade*, CERN-LHCC-2012-007 (2012).
[26] R. Aaij *et al.*, Eur. Phys. J. C **73** (2013) 2373 [arXiv:1208.3355 [hep-ex]].